Synthesis and Properties of Indeno[2,1-c]fluorenes and Benzo- Fused Analogues

Tanguy Jousselin-Oba, Parker E Deal, Aaron G Fix, Conerd K Frederickson, Chris L Vonnegut, Abderrahim Yassar, Lev N Zakharov, Michel Frigoli, Michael M Haley

Synthesis and Properties of Indeno[2,1-*c*]fluorenes and Benzo-Fused Analogues

Tanguy Jousselin-Oba,[a] Parker E. Deal,[b] Aaron G. Fix,[b] Conerd K. Frederickson,[b] Chris L. Vonnegut,[b] Abderrahim Yassar,[c] Lev N. Zakharov,[d] Michel Frigoli,*[a] and Michael M. Haley*[b]

Abstract: A new set of fully-conjugated indenofluorenes has been synthesized and confirmed by solid-state structure analysis. The indeno[2,1-*c*]fluorenes and their benzo-fused analogues all contain the antiaromatic *as*-indacene core. The molecules possess high electron affinities and show a broad absorption that reaches into the near-IR region of the electromagnetic spectrum. All of the featured compounds reversibly accept up to two electrons as revealed by cyclic voltammetry. Analysis of molecule tropicity using NICS-XY scan calculations show that, while the *as*-indacene core is less paratropic than *s*-indacene, benz[a]-annulation further reduces the antiaromaticity of the core. Antiaromatic strength of the *as*-indacene core can also be tuned by the position of fusion of additional arenes on the outer rings.

Introduction

Organic semiconductors (OSCs) have been the subject of intense academic and industrial research for several decades, comprising one of the most significant areas of study in materials chemistry. Such allure is to be expected as semiconductors are fundamental to the construction of electronic devices now ubiquitous in modern society.[1] With a drive to make devices that we utilize every day more energy-efficient and user friendly, there has been significant research effort focused on developing organic electronic materials for niche applications, such as wearable devices and flexible display technologies that will consume a fraction of the energy of those in use today.[2] To make this transition from the research laboratory to commercial application feasible, one of the main directives of this research area has been to develop new OSCs that are solution-processible, possess robust operational stability to common environmental contaminants/doping, are relatively cheap and easy to manufacture, are easily functionalized/tuned in the final synthetic step(s), etc.[2,3] Acenes and other related polycyclic aromatic hydrocarbons (PAHs) have been studied intensively in this regard.[4] Of particular interest in the search for organic electronic materials are the cyclopenta-fused PAHs[5] (CP-PAHs, e.g., fullerenes,[6] buckybowls,[7] etc.), as the five-membered ring(s) within these compounds impart a higher electron affinity because of the driving force to aromatize to a cyclopentadienyl anion by accepting an electron.[5]

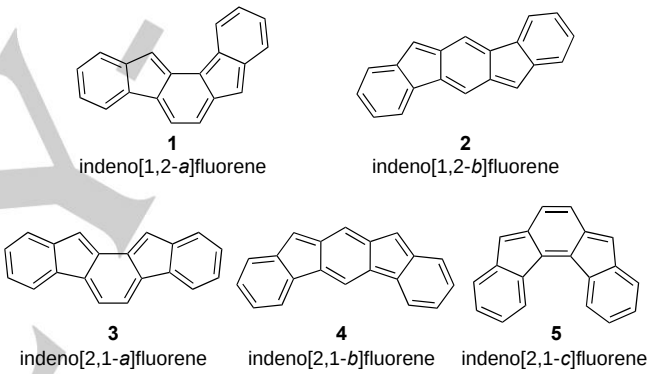

Figure 1. The five possible indenofluorene regioisomers **1**–**5**.

Our work within this class of molecules has focused mainly on the fully conjugated indenofluorenes (IFs),[8] a family of cyclopenta-fused hydrocarbons comprised of five structural isomers (**1**–**5**, Figure 1).[9] Although known since 1957,[10] these π-electron-rich compounds were essentially ignored over the subsequent 50+ years.[11] In 2011 we reported the synthesis and structural characterization of stable ethynylated derivatives of [1,2-*b*]IF (**2**)[12] and showed that such molecules could be used as OSCs in ambipolar OFETs.[13] This area has since seen tremendous growth with 150+ published studies on indenofluorenes and related diindenoacene/diarenoindacene topologies. All five regioisomers are now known, culminating in 2017 with the identification of the [1,2-*a*]IF scaffold (**1**).[14] Like the [2,1-*b*]IF (**4**) derivative prepared by Tobe in 2013,[15] IF **1** exhibits a high degree of diradical character, making it (and **4**) rather unstable. On the other hand, IF regioisomers **2**, **3**, and **5** possess considerably reduced diradical character; thus, stable derivatives can be prepared by inclusion of bulky and/or electron-withdrawing groups on the apical carbons of the five-membered rings, i.e., the sites of greatest spin density.[8]

We have been pursuing two complementary strategies for tailoring the electronic properties of our CP-PAHs, namely (1) elongation of the quinoidal central core while maintaining the

[a] T. Jousselin-Oba, Dr. M. Frigoli
UMR CNRS 8180, Institut Lavoisier de Versailles
UVSQ, Université Paris-Saclay
45 Avenue des Etats-Unis, 78035 Versailles Cedex, France
E-mail: michel.frigoli@uvsq.fr
[b] P. E. Deal, Dr. A. G. Fix, Dr. C. K. Frederickson, Dr. C. L. Vonnegut, Prof. M. M. Haley
Department of Chemistry & Biochemistry and Materials Science Institute
1253 University of Oregon
Eugene, Oregon 97403-1253, United States
E-mail: haley@uoregon.edu
[c] Dr. A. Yassar
UMR CNRS 7647, LPICM-École Polytechnique
91128 Palaiseau Cedex, France
[d] Dr. L. N. Zakharov
CAMCOR – Center for Advanced Materials Characterization in Oregon
University of Oregon
Eugene, Oregon 97403-1433, United States

Supporting information for this article is given via a link at the end of the document.

same fused outer ring[16] and (2) variation of the fused outer ring while retaining the same core motif.[17] This latter strategy is the easier of the two as synthesis of the requisite dione precursors is in general relatively straightforward. While a majority of the reported studies have focused on [1,2-*b*]IF **2** and other closely related D_{2h}-symmetrical diindenoacenes, we disclosed the initial foray into the C_{2v}-symmetric [2,1-*c*]IF scaffold in 2013.[18] Given our recent study on benzo-fused [1,2-*b*]IFs,[17c] we decided to reinvestigate this particular regioisomer. Herein we report the synthesis and characterization of the new benzo-fused congeners **6**-**8** and compare their optical and electronic properties with previously reported derivatives **5a**-**5c**.

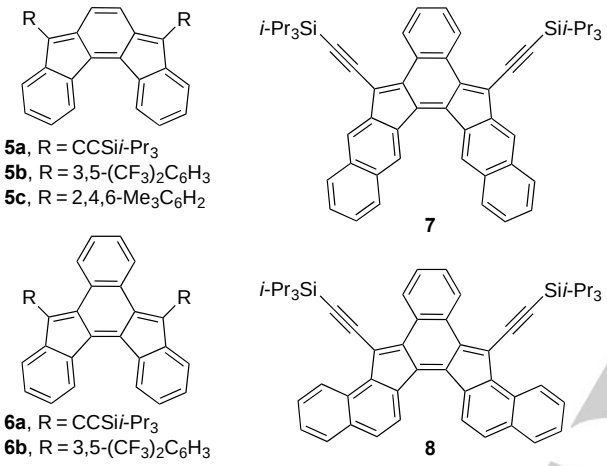

Figure 2. Indeno[2,1-*c*]fluorene derivatives described in this study.

Results and Discussion

Synthesis. Diones **9**[19] and **10**,[20] the precursors of **5** and **6**, respectively, can be prepared via the previously reported pathway of Diels-Alder cycloaddition of the requisite cyclopentadienone followed by cheletropic elemination of CO and then "inside-out" Friedel-Crafts acylation onto the outer benzenes. Alternatively, we explored the "outside-in" Friedel-Crafts route as well to avoid the sometimes-difficult task of cyclopentadienone formation. As shown in Scheme 1, Suzuki cross-coupling of naphthalene **11**[21] to ester **12** furnished diester **13**, which could be cyclized with TfOH[22] to give dione **10**. Addition of the lithiated nucleophile to either **9** or **10** followed by $SnCl_2$-mediated reductive dearomatization[23] of the central arene afford the desired [2,1-*c*]IF derivatives as green-black solids. Whereas the $SnCl_2$ reaction proceeded smoothly at room temperature for **5a** and **6a**, the addition of catalytic TFA with moderate heating (50-80 °C) was necessary for the successful generation of the arylated systems. It should be noted that we did try to prepare **6c** in analogy to **5c**; however, we were unable to perform a successful reductive dearomatization on the intermediate diol.

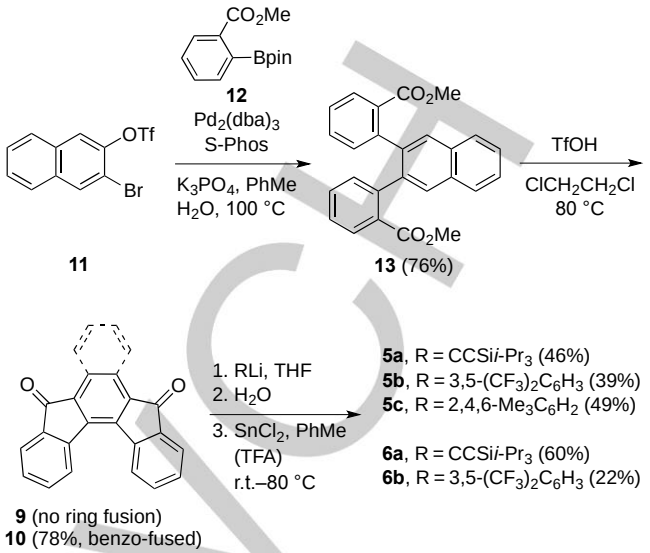

Scheme 1. Synthesis of Indeno[2,1-*c*]fluorenes **5a**-**c** and **6a**-**b**.

The synthesis of unknown diones **14** and **15**, the precursors of IFs **7** and **8**, respectively, also followed the "outside-in" Friedel-Crafts pathway. Starting again from **11**, Suzuki cross-coupling with ester **16**[24] afforded diester **17**, which underwent Friedel-Crafts acylation using TfOH to furnish **14** (Scheme 2). Addition of lithium (triisopropylsilyl)acetylide and subsequent reductive dearomatization with $SnCl_2$ gave the fully conjugated [2,1-*c*]IF **7** in good overall yield.

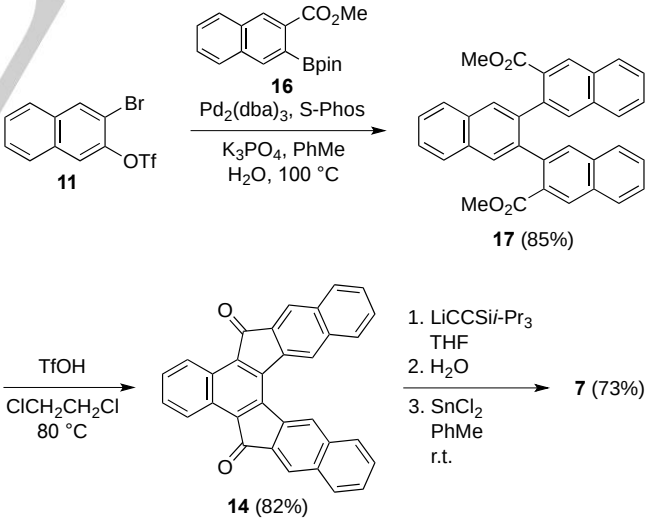

Scheme 2. Synthesis of Indeno[2,1-*c*]fluorene **7** via Dione **14**.

To our surprise, attempts to perform the analogous double Suzuki cross-coupling on **11** using isomeric ester **18**[25] were not successful; thus, a revised synthesis is shown in Scheme 3 where each indene unit is introduced in a stepwise manner.

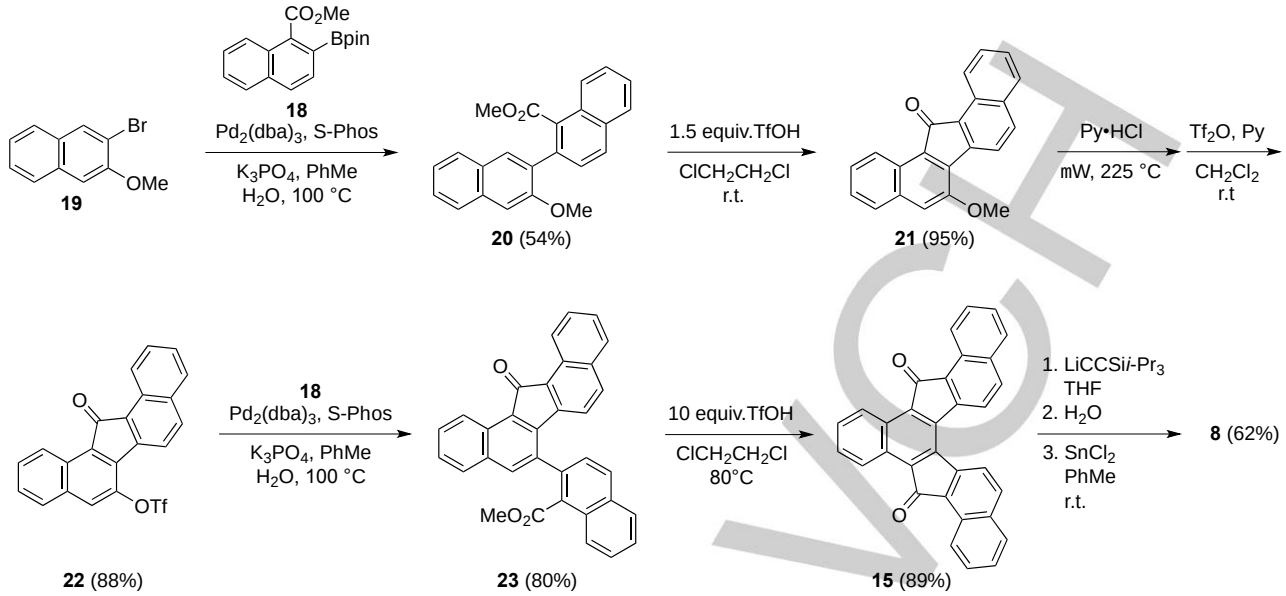

Scheme 3. Synthesis of Indeno[2,1-*c*]fluorene **8** via Dione **15**.

Cross-coupling **18** to 2-bromo-3-methoxynaphthalene (**19**) gave **20**, which could be cyclized with TfOH to furnish ketone **21**. Demethylation with Py•HCl and then triflate formation provided **22**. A second Suzuki cross-coupling with **18** and again Friedel-Crafts acylation using TfOH gratifyingly furnished dione **15**. Addition of lithium (triisopropylsilyl)acetylide and subsequent reductive dearomatization with $SnCl_2$ gave the fully conjugated [2,1-*c*]IF **8** in good overall yield. Unfortunately, attempts to prepare the third naphtho-fused regioisomer were unsuccessful, likely because of severe steric crowding. Similarly, attempts to prepare the analogue of **14** minus the benz[*a*]-fusion afforded a mixed 5-6-7-membered ring product and not the desired dione.

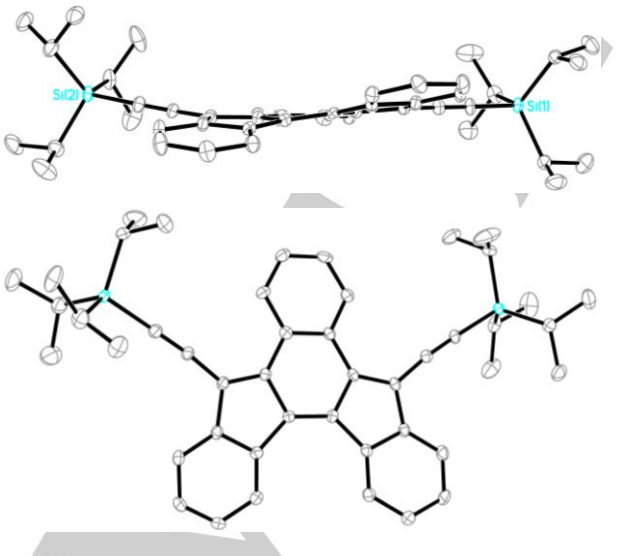

Figure 3. Side and top view of the X-ray structure of **6a**. Ellipsoids drawn at the 30% probability level and hydrogens omitted for clarity.

X-ray analysis. Single crystals of **6a** suitable for X-ray diffraction were obtained via slow crystallization from toluene. The resultant crystal structure (Figure 3) shows that the molecule possesses a slight helicene-like axial chirality, with equal occupancy between the *M*- and *P*-isomers.[26] The dihedral angles between the average planes of the central six-membered ring, the bridging five-membered ring, and the terminal six-membered ring of **6a** are 5.5/7.0° and 6.2/7.6°, respectively, values that are slightly larger than those found in the X-ray structure of **5c** (*P*-isomer: 2.3/4.3° and 2.0/2.4°; *M*-isomer: 4.8/6.6° and 4.7/3.7°).[18] Nonetheless, the barrier to inversion is extremely small as no appreciable line broadening is observed in the proton NMR spectrum upon cooling. The molecules pack as essentially isolated molecules (i.e., no cofacial stacking) with only a single close intermolecular C–C contact of 3.42 Å.

Comparison of the bond lengths in **6a** with those in the two independent molecules of **5a** clearly shows the effect of benz[*a*]-fusion to the [2,1-*c*]IF core (Table 1). Most affected is bond a, which lengthens by ~0.06 Å from 1.355-1.359 Å in **5c** to 1.418 Å in **6a**, the latter value typical of the fused arene bond in adjoining rings, *cf.* bond g. Bond b lengthens a more modest ~0.015-0.025 Å because of its (now) benzylic nature, whereas nearly all of the remaining bond lengths are essentially the same between the two structures (i.e., a benzo-fused biindenylidene). To minimize steric interactions with the bulky TIPS groups, the triple bonds bend away from the 'bay' region C–H units ca. 1.4-6.3° from the preferred linearity of *sp*-hybridized carbon atoms.

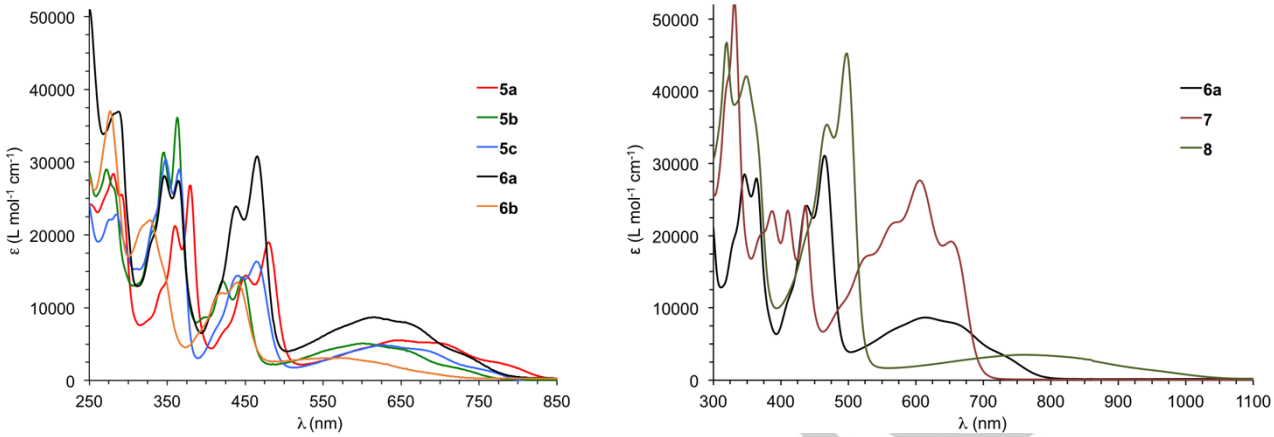

Figure 4. Electronic absorption spectra of (left) **5a**-**c** and **6a**-**b** in CH_2Cl_2 and (right) **6a**, **7**, and **8** in $CHCl_3$.

Table 1. Select Bond Lengths (Å) of [2,1-c]IFs **5c** and **6a**.

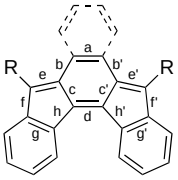

bond	**5c-*P*** [a]	**5c-*M*** [a]	**6a**
a	1.359(2)	1.355(2)	1.418(6)
b	1.428(2)	1.439(2)	1.452(6)
b'	1.434(2)	1.433(2)	1.460(5)
c	1.472(2)	1.468(2)	1.462(5)
c'	1.471(2)	1.469(2)	1.462(5)
d	1.367(2)	1.364(2)	1.364(6)
e	1.371(2)	1.370(2)	1.384(5)
e'	1.371(2)	1.377(2)	1.376(5)
f	1.468(2)	1.464(2)	1.471(2)
f'	1.464(2)	1.461(2)	1.471(2)
g	1.414(2)	1.413(2)	1.413(2)
g'	1.415(2)	1.419(2)	1.413(2)
h	1.482(2)	1.474(2)	1.469(3)
h'	1.483(2)	1.475(2)	1.469(3)

[a] Reference [18].

Electronic absorption data. The UV-vis spectra of **5a-c**, **6a**-**b**, **7** and **8** (Figure 4) display strong absorbances in the higher energy range and a broad low-energy absorbance stretching out to the near-IR region (550-1050 nm). It is noteworthy that the weak low-energy bands in the [2,1-*c*]IF derivatives are similarly observed in the spectrum of 11,12-dimesityl[2,1-*a*]IF (based on **3**),[27] which also possesses the *as*-indacene core. This is in contrast to the spectra of [1,2-*b*]IFs, which are based on the *s*-indacene skeleton, as the λ_{max} of the lowest energy peak of the derivatives of **2** to date has been less than 615 nm.[12,13] Calculations revealed that the source of the low energy bands in the C_{2v}-symmetric [2,1-*c*]IF core is an allowed HOMO→LUMO (π→π*) transition, whereas this same transition is forbidden in the D_{2h}-symmetric [1,2-*b*]IF skeleton.[28]

Comparison of the data for **5** and **6** readily show the effect of benz[*a*]-annulation, in that the absorption bands blue-shift by roughly 15-30 nm (Figure 4, Table 2) as do the absorption cut-offs up to 50 nm, indicating decreased conjugation within the *as*-indacene core. On the other hand, analogous benzannulation of the [2,1-*a*]IF scaffold produces a 250 nm red-shift between the spectra (800→1050 nm); however, unlike **6** where the x-ray data show the extra ring to be a fused benzene (*vide supra*), the x-ray data of the benz[*c*]indeno[2,1-*a*]fluorene derivative indicate the new ring to be quinoidal and thus the core is highly conjugated.[28] Within the ethynylated benz[*a*]-series of **6a**, **7** and **8**, linear fusion in **7** with two additional benzene rings further blue-shifts the bands, with the absorption cut-off almost 100 nm shorter, whereas angular fusion in **8** affords a 250 nm red-shift in its spectrum (800→1050 nm). We believe this is due to a strong intramolecular charge transfer from the HOMO to the LUMO MOs, which should be less pronounced in **6a** and essentially non-existent in **7**. These latter results are in contrast to the same experiments in the naphtho-fused *s*-indacenes, where the additional two benzene rings always resulted in a red-shift of the absorption bands regardless of the mode of ring fusion.[17c] Nonetheless, as noted above, the low energy bands observed for the [2,1-*c*]IF core are forbidden for the [1,2-*b*]IFs; therefore, direct comparison of the UV-vis results between the various IF skeletons may not entirely be valid. Similar to other fully conjugated IFs, compounds **5**-**8** are non-emissive due to rapid non-radiative decay via a conical intersection.[29]

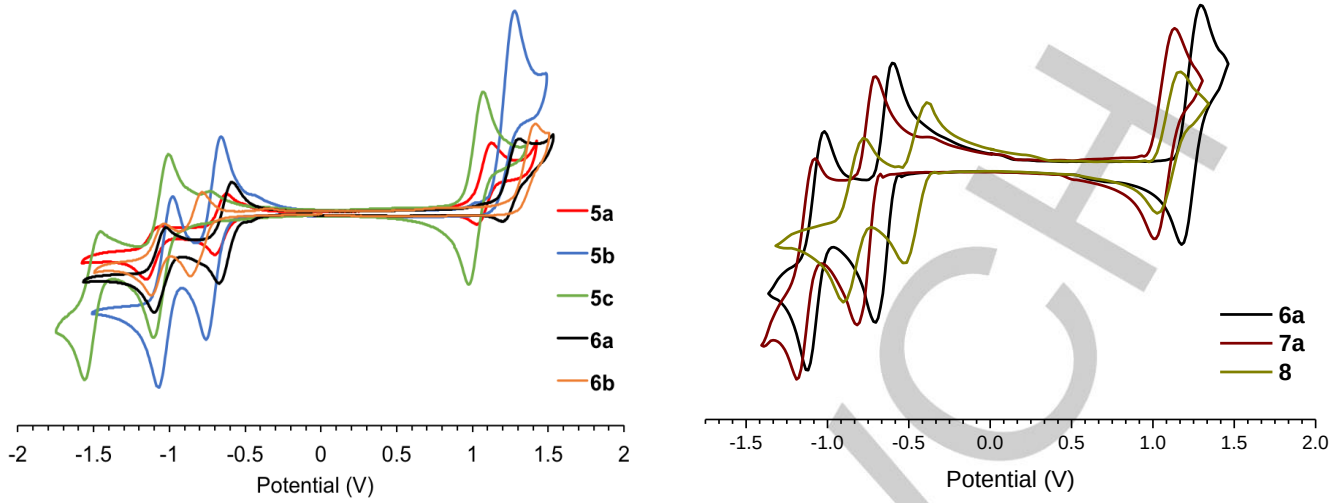

Figure 5. Cyclic voltammograms of (left) **5a**-**c** and **6a**-**b** and (right) **6a**, **7**, and **8** in CH_2Cl_2.

Table 2. Summary of optical and electrochemical data of compounds **5–8**

	electrochemical						optical	
Cmpd	E_{red}^1 (V)	E_{red}^2 (V)	E_{ox} (V)	E_{LUMO} (eV)	E_{HOMO} (eV)	E_{gap} (eV)	λ_{max} (nm)	E_{gap} (eV)[c]
5a[a]	–0.66	–1.11	1.07	–3.98	–5.71	1.73	360, 380, 451, 480, 647	1.49
5b[a]	–0.71	–1.02	—- [d]	–3.93	—	—	348, 365, 441, 465, 627	1.60
5c[a]	–1.05	–1.51	1.02	–3.59	–5.66	2.08	345, 363, 421, 447, 603	1.54
6a[a]	–0.63	–1.06	1.25	–4.01	–5.89	1.87	347, 364, 438, 465, 615	1.57
6b[a]	–0.82	–1.08	—- [d]	–3.82	—	—	328, 419, 440, 571	1.68
6a[b]	–1.16	–1.58	0.73	–3.64	–5.53	1.89	347, 364, 438, 465, 615	1.57
7[b]	–1.27	–1.64	0.56	–3.53	–5.36	1.83	331, 387, 411, 437, 606, 654	1.78
8[b]	–0.96	–1.35	0.59	–3.84	–5.39	1.55	320, 348, 468, 498, 764	1.24

[a] CV recorded in Oregon using 1-5 mM of analyte in 0.1 M Bu_4NOTf/CH_2Cl_2 using a scan rate of 50 mV s^{-1}. The working electrode was a glassy carbon electrode with a Pt coil counter electrode and Ag wire pseudoreference. Values reported as the half-wave potential (vs SCE) using the Fc/Fc^+ couple (0.46 V) as an internal standard; see reference [30]. Energy levels were approximated by $E_{LUMO} = -(4.68 + E_{red}^1)$ and $E_{HOMO} = -(4.68 + E_{ox}^1)$; see reference [31]. [b] CV recorded in France using 1-2 mM of analyte in 0.1 M Bu_4NPF_6/CH_2Cl_2 using a scan rate of 100 mV s^{-1}. The working electrode was a glassy carbon electrode with a Pt coil counter electrode and Ag/AgCl (EtOH) as pseudo reference electrode. Values reported as the half-wave potential (vs Fc/Fc^+) using the Fc/Fc^+ couple (0.51 V) as an internal standard. Energy levels determined by $E_{LUMO} = -(4.8 + E_{red}^1)$ and $E_{HOMO} = -(4.8 + E_{Ox}^1)$. [c] The optical HOMO-LUMO energy gap was determined as the intersection of the x-axis and a tangent line that passes through the inflection point of the lowest energy absorption. [d] Reversible oxidation was not achieved.

Electrochemistry. Cyclic voltammograms (CV) of molecules **5**-**8** are shown in Figure 5 and the results compiled in Table 2. The CV data indicate that like the [1,2-*b*]IFs (**2**) and [2,1-*a*]IFs (**3**), the family of [2,1-*c*]IFs is electron deficient. The compounds can reversibly accept up to two electrons and possess LUMO energies estimated at –3.5 to –4.0 eV, analogous to those found in derivatives of **2**;[12b,13a] however, the HOMO energies of **5** are roughly 0.15 eV higher, thus leading to reduced gap energies compared to their identically substituted analogues of **2** (e.g., 1.89 eV for **2a** vs 1.73 eV for **5a**).[12b] Benz[*a*]-fusion appears to lower the HOMO energy level back close to **2** such that energy gaps are nearly identical (e.g., 1.89 eV for **2a** vs. 1.87 eV for **6a**). Unlike the absorption data, inclusion of the two additional benzene rings in **7** and **8** lowers the energy gap to 1.83 and 1.55 eV, respectively, regardless of the mode of ring fusion and thus the CV results closely parallel those obtained for the naphtho-fused *s*-indacene congeners (energy gap of 1.75 and 1.57 eV, respectively).[17c]

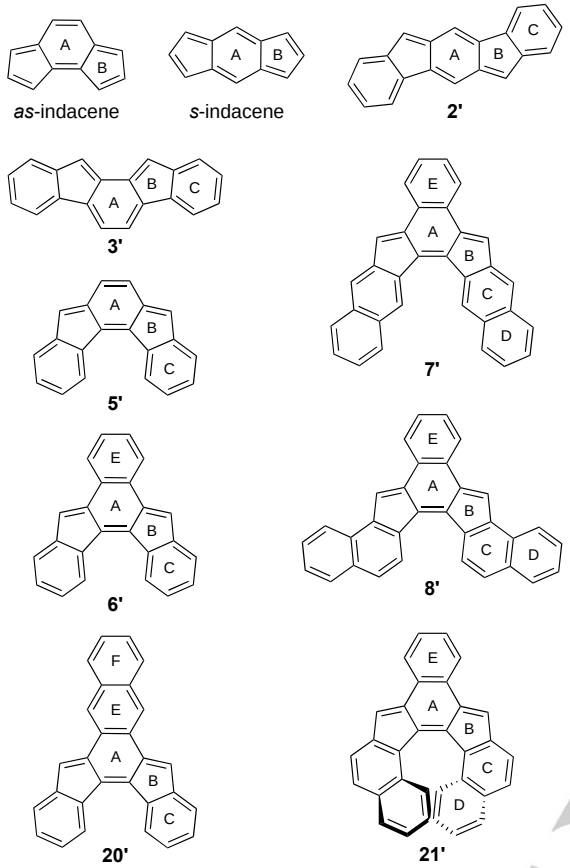

Figure 6. Structures for comparison in the NICS-XY scan computations; lettering corresponds to ring assignments in Figure 7 and Table 3.

NICS-XY Scan Calculations. To compare the effects of benzo-fusion on the aromaticity/antiaromaticity of the indeno[2,1-*c*]fluorene skeleton, as well as to compare the three closed-shell IF regioisomers, we performed nucleus independent chemical shift (NICS) computations on the structures shown in Figure 6 using the NICS-XY scan and π-only methods.[32] Parent versions of each compound without the mesityl or alkynyl groups on the five-membered rings were used to simplify comparisons as well as make the most efficient use of computational resources; prior results have also shown that inclusion of these groups in the computed structures has minimal effect on the outcome of the NICS-XY scans.[16c,17c] Our initial assessment led to some surprising results, in that the NICS-XY scans were lopsided. Although not too evident in the scans for **5'**, **6'** and **20'**, the results for **7'**, **8'** and especially **21'** were noticeably misshapen (see Supporting Information, Figure S1). As noted earlier, the [2,1-*c*]IF geometry is helical, and this helicity is exacerbated in **21'**, where the ghost atom at the end of the NICS-XY scan ends up essentially underneath the top ring (Figure S2), thus making it difficult to parse out the actual $NICS_{\pi ZZ}$ value for that ring. Despite their helicity, these molecules still are symmetric; therefore, we can create a good approximation of the full graph by taking the first half of the scan where the points are on top of the molecule, i.e., uncontaminated by proximity to other parts of the molecule, and mirror the results. The resultant plots (Figure 7) resemble those of the [1,2-*b*]IF derivatives.[17c] The $NICS_{\pi ZZ}$ values for each ring are summarized in Table 3.

Table 3. Summary of $NICS_{1.7\pi ZZ}$ values

	Ring[a]					
cmpd	A	B	C	D	E	F
as-ind	14	23				
s-ind	23	26				
2'	5	7	–9			
3'	6	10	–8			
5'	3	9	–10			
6'	1	7	–11		–13	
7'	0	4	–12	–16	–13	
8'	4	11	–12	–15	–11	
20'	1	6	–12		–14	–16
21'	4	12	–13	–16	–11	

[a] Ring assignments shown in Figure 6.

As shown in Figure 7a, the NICS-XY scans reveal that *as*-indacene (teal) is less antiaromatic than *s*-indacene (fuchsia), especially in the central 6-membered ring (14 vs. 23 ppm, ring A in Table 3). Nonetheless, fusion of the outer benzenes (ring C) to create the indenofluorene skeleton essentially negates this difference, as the chemical shift values for the ghost atoms now vary less than 2.5 ppm, i.e., all three IF isomers are comparable in their moderate-to-weak paratropicity and moderately strong diatropicity in the indacene core and outer benzenes, respectively. Fusion of a third arene in the benz[*a*]-position of **5'** (ring E) further reduces indacene paratropicity and slightly increases benzene ring C diatropicity (Figure 7b) in **6'** and **20'** by ca. 2-3 ppm. Performing the NICS-XY scan along the axis of benz[*a*]-fusion (Figure 7c) illustrates that there is little difference in the central 6-membered ring A of the indacene as one changes from benzo- (**6**) to naphtho-fusion (**20**). 1,2-Naphtho-fusion (e.g., **8'**, **21'**) does increase indacene paratropicity by ca. 3 ppm; nonetheless, rings C and D become progressively more aromatic, which is reflected in the chemical shift values in **7'**, **8'** and **21'** (Figure 7d) from –11/–13 ppm to –14/–16 ppm. Analogous to the [1,2-*b*]IF congeners,[17c] these naphtho-fused derivatives show the same trend within the indacene core: derivatives having a lower bond order of ring fusion (e.g., **7'**, bond order of 1.33) display reduced internal paratropicity strength, whereas derivatives having a higher bond order of ring fusion (e.g., **8'** and **21'**, bond order of 1.66) exhibit increased internal paratropicity strength, when both are compared to **6** (bond order of 1.5). As might be expected based on our DNI studies (*vide supra*),[17c] compound **8** is easier to reduce than **7** because of its larger paratropicity.

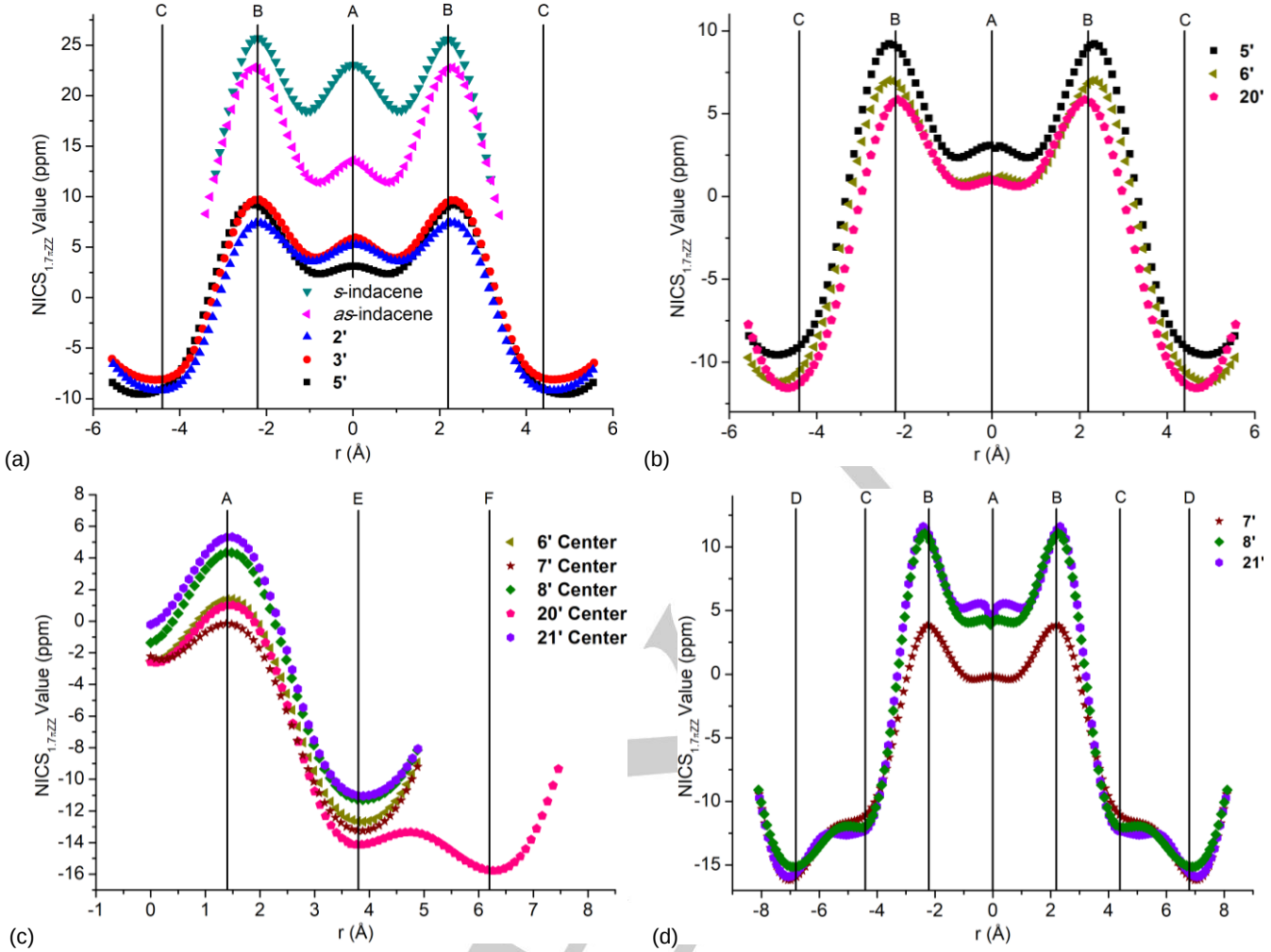

Figure 7. NICS$_{\pi ZZ}$-XY scans of (a) *as*- and *s*-indacene and IFs **2'**, **3'** and **5'**, (b) IFs **5'**, **6'** and **20'** along the pentacyclic core, (c) IFs **6'**-**8'** and **20'**-**21'** along the axis of benz[*a*]-fusion, and (d) IFs **7'**, **8'** and **21'** along the heptacyclic core. The vertical lines correspond to the ring centers labeled in Figure 6.

Conclusions

Benzo-fused analogues of the indeno[2,1-*c*]fluorene skeleton containing the *as*-indacene core have been synthesized. The addition of the extra benzene ring enables the variation of the annelation mode and has been achieved by two different routes. The benzo[*a*]-fusion reduces slightly the energy band gap without altering the high electron affinity of the π-system (comparison **5a**/**6a**). In contrast to the indeno[1,2-*b*]fluorene family, the absorption behavior of the [2,1-*c*]IFs displays allowed low-energy transitions in the near-IR region and the electron acceptability increases with increasing paratropicity of the system. Remarkably, dinaphtho-*as*-indacene **8** has the highest electron affinity, an absorption maximum at 762 nm with a lambda edge up to 1050 nm, and could behave as an ambipolar semiconductor. Among all diacenoindacenes with a closed-shell configuration in the ground state synthesized to date,[8] compound **8** is unique to surpass 1000 nm of the near-IR region. Future studies will examine other modes of annelation upon the indeno[2,1-*c*]fluorene scaffold.

Acknowledgements

We thank the National Science Foundation (CHE-1565780) to M.M.H. and Agence nationale de la recherché (ANR-16-CE07-0024 GATE) to M.F. for support of this research. Mass spectrometry capabilities in the CAMCOR facility are supported by the NSF (CHE-1625529).

Keywords: indenofluorenes • diacenoindacenes • Friedel-Crafts acylation • antiaromaticity • NICS calculations

[1] a) S. M. Sze, *Semiconductor Devices: Physics and Technology*, Wiley: New York, NY, **2002**; b) S. R. Forrest. *Nature* **2004**, *428*, 911–918; c) H. E. Katz, J. Huang. *Annu. Rev. Mater. Res.* **2009**, *39*, 71–92; d) F. M. Li, A. Nathan, Y. Wu, B. S. Ong, *Organic Thin Film Transistor Integration: A Hybrid Approach*; Wiley-VCH: Weinheim, Germany, **2011**; e) *Semiconductor Nanomaterials for Flexible Technologies: From Photovoltaics and Electronics to Sensors and Energy Storage*; Eds.: Y. Sun, J. A. Rogers; William Andrew Publishing: Oxford, UK, **2010**.

[2] a) Y. Zhou, C. Fuentes-Hernandez, J. Shim, J. Meyer, A. J. Giordano, H. Li, P. Winget, T. Papadopoulos, H. Cheun, J. Kim, M. Fenoll, A.

Dindar, W. Haske, E. Najafabadi, T. M. Khan, H. Sojoudi, S. Barlow, S. Graham, J.-L. Brédas, S. R. Marder, A. Khan, B. Kippelen, *Science* **2012**, *336*, 327–332; b) J. Lambrecht, T. P. I. Saragi, J. Salbeck, *J. Mater. Chem.* **2011**, *21*, 18266–18270; c) T. Sekitani, T. Yokota, U. Zschieschang, H. Klauk, S. Bauer, K. Takeuchi, M. Takamiya, T. Sakurai, T. Someya, *Science* **2009**, *326*, 1516–1519; d) M. Irimia-Vladu, N. S. Sariciftci, S. Bauer, *J. Mater. Chem.* **2011**, *21*, 1350–1361.

[3] a) J. Mei, Y. Diao, A. L. Appleton, L. Fang, Z. Bao, *J. Am. Chem. Soc.* **2013**, *135*, 6724–6746; b) J. E. Anthony, A. Facchetti, M. Heeney, S. R. Marder, X. Zhan, *Adv. Mater.* **2010**, *22*, 3876–3892.

[4] a) M. Bendikov, F. Wudl, D. F. Perepichka, *Chem. Rev.* **2004**, *104*, 4891–4946; b) J. E. Anthony, *Chem. Rev.* **2006**, *106*, 5028–5048; c) J. E. Anthony, *Angew. Chem. Int. Ed.* **2008,** *47*, 452–483; *Angew. Chem.* **2008,** *120*, 460–492.

[5] a) G. E. Rudebusch, M. M. Haley, in *Polycyclic Arenes and Heteroarenes: Synthesis, Properties and Applications*, Ed.: Q. Miao, Wiley-VCH: Weinheim, **2015**, pp. 37–60; b) J. L. Marshall, M. M. Haley, in *Organic Redox Systems: Synthesis, Properties and Applications*, Ed.: T. Nishinaga, John Wiley & Sons: New York, **2016**, pp. 311–358; c) K. N. Plunkett, *Synlett* **2013**, *24*, 898–902; d) H. Hopf, *Angew. Chem. Int. Ed.* **2013**, *52*, 12224–12226; *Angew. Chem* **2013**, *125*, 12446–12449.

[6] *Fullerenes: Principles and Applications*, Eds.: F. Langa, J.-F. Nierengarten, Royal Society of Chemistry: Cambridge, UK, **2011**.

[7] a) L. T. Scott, *Polycyclic Aromat. Cmpd.* **2010**, *30*, 247–259; b) *Fragments of Fullerenes and Carbon Nanotubes. Designed Synthesis, Unusual Reactions, and Coordination Chemistry*, Eds.: M. A. Petrukhina, L. T. Scott, John Wiley & Sons: Hoboken, NJ, **2011**.

[8] C. K. Frederickson, B. D. Rose, M. M. Haley, *Acc. Chem. Res.* **2017**, *50*, 977–987.

[9] A. G. Fix, D. T. Chase, M. M. Haley, *Top. Curr. Chem.* **2014**, *349*, 159–195.

[10] A. LeBerre, *Ann. Chim.* **1957**, *2*, 371–423.

[11] a) Q. Zhou, P. J. Carroll, T. M. Swager, *J. Org. Chem.* **1994**, *59*, 1294–1301; b) H. Reisch, U. Wiesler, U. Scherf, N. Tuytuylkov, *Macromolecules* **1996**, *29*, 8204–8210.

[12] a) D. T. Chase, B. D. Rose, S. P. McClintock, L. N. Zakharov, M. M. Haley, *Angew. Chem. Int. Ed.* **2011**, *50*, 1127–1130; *Angew. Chem.* **2011**, *123*, 1159–1162; b) D. T. Chase, A. G. Fix, B. D. Rose, C. D. Weber, S. Nobusue, C. E. Stockwell, L. N. Zakharov, M. C. Lonergan, M. M. Haley, *Angew. Chem. Int. Ed.* **2011**, *50*, 11103–11106; *Angew. Chem.* **2011**, *123*, 11299–11302.

[13] a) D. T. Chase, A. G. Fix, S. J. Kang, B. D. Rose, C. D. Weber, Y. Zhong, L. N. Zakharov, M. C. Lonergan, C. Nuckolls, M. M. Haley, *J. Am. Chem. Soc.* **2012**, *134*, 10349–10352; b) see also: J. Nishida, S. Tsukaguchi, Y. Yamashita, *Chem. Eur. J.* **2012**, *18*, 8964–8970.

[14] J. J. Dressler, Z. Zhou, J. L. Marshall, R. Kishi, S. Takamuku, Z. Wei, S. N. Spisak, M. Nakano, M. A. Petrukhina, M. M. Haley, *Angew. Chem. Int. Ed.* **2017**, *56*, 15363–15367; *Angew. Chem.* **2017**, *129*, 15565–15569.

[15] a) A. Shimizu, R. Kishi, M. Nakano, D. Shiomi, K. Sato, T. Takui, I. Hisaki, M. Miyata, Y. Tobe, *Angew. Chem. Int. Ed.* **2013**, *52*, 6076–6079; *Angew. Chem.* **2013**, *125*, 6192–6195; b) see also: Y. Tobe, *Chem. Rec.* **2015,** *15*, 86–96.

[16] Inter alia: a) G. E. Rudebusch, A. G. Fix, H. A. Henthorn, C. L. Vonnegut, L. N. Zakharov and M. M. Haley, *Chem. Sci.* **2014**, *5*, 3627–3633; b) K. Sbargoud, M. Mamada, J. Marrot, S. Tokito, A. Yassar, M. Frigoli, *Chem Sci.* **2015**, *6*, 3402–3409; c) G. E. Rudebusch, J. L. Zafra, K. Jorner, K Fukuda, J. L. Marshall, I. Arrechea-Marcos, G. L. Espejo, R. P. Oritz, C. J. Gómez-García, L. N. Zakharov, M. Nakano, H. Ottosson, J. Casado, M. M. Haley, *Nat. Chem.* **2016**, *8*, 753–759; d) J. E. Barker, C. K. Frederickson, M. H. Jones, L. N. Zakharov and M. M. Haley, *Org. Lett.* **2017**, *19*, 5312–5315.

[17] Inter alia: a) B. S. Young, D. T. Chase, J. L. Marshall, C. L. Vonnegut, L. N. Zakharov and M. M. Haley, *Chem. Sci.* **2014**, *5*, 1008–1014; b) J. L. Marshall, K. Uchida, C. K. Frederickson, C. Schutt, A. M. Zeidell, K. P. Goetz, T. W. Finn, K. Jarolimek, L. N. Zakharov, C. Risko, R. Herges, O. D. Jurchescu, M. M. Haley, *Chem. Sci.* **2016**, *7*, 5547–5558; c) C. K. Frederickson, L. N. Zakharov and M. M. Haley, *J. Am. Chem. Soc.* **2016**, *138*, 16827–16838; d) J. J. Dressler, M. Teraoka, G. L. Espejo, R. Kishi, S. Takamuku, C. J. Gomez-Garcia, L. N. Zakharov, M. Nakano, J. Casado, M. M. Haley, *Nat. Chem.* **2018**, *10*, in press/online; e) C. K. Frederickson, J. E. Barker, Z. Zhou, J. J. Dressler, E. R. Hanks, J. P. Bard, L. N. Zakharov, M. A. Petrukhina, M. M. Haley, *Synlett* **2018**, *29*, in press/online.

[18] A. G. Fix, P. E. Deal, C. L. Vonnegut, B. D. Rose, L. N. Zakharov, M. M. Haley, *Org. Lett.* **2013**, *15*, 1362–1365.

[19] a) L. G. Scanlon, W. A. Feld, P. B. Balbuena, G. Sandi, X. Duan, K. A. Underwood, N. Hunter, J. Mack, M. A. Rottmayer, M. Tsao, *J. Phys. Chem. B* **2009**, *113*, 4708–4717; b) K. Underwood, M.Sc. Thesis, Wright State University, Dayton, OH, **2006**.

[20] Y. Yang, J. L. Petersen, K. K. Wang, *J. Org. Chem.* **2003**, *68*, 5832–5837.

[21] J. Shao, X. Zhao, L. Wang, Q. Tang, W. Li, H. Yu, H. Tian, X. Zhang, Y. Geng, F. Wang, *Tetrahedron Lett*. **2014**, *55*, 5663–5666.

[22] T. Jousselin-Oba, K. Sbargoud, G. Vaccaro, F. Meinardi, A. Yassar, M. Frigoli, *Chem. Eur. J.* **2017**, *23*, 16184–16188.

[23] J. L. Marshall, D. Lehnherr, B. D. Lindner, R. R. Tykwinski, *ChemPlusChem* **2017**, *82*, 967–1001.

[24] Y. Xia, Z. Liu, Q. Xiao, P. Qu, R. Ge, Y. Zhang, J. Wang, *Angew. Chem. Int. Ed.* **2012**, *51*, 5714–5717; *Angew. Chem.* **2012**, *124*, 5812–5815.

[25] B. Ghaffari, S. M. Preshlock, D. L Plattner, R. J Staples, P. E. Maligres, S. W. Krska, R. E. Maleczka Jr., M. R. Smith, *J. Am. Chem. Soc.* **2014**, *136*, 14345–14348.

[26] CCDC 1873497 contains the supplementary crystallographic data for compound **6a**. These data can be obtained free of charge from the Cambridge Crystallographic Data Centre via www.ccdc.cam.ac.uk/data_request/cif

[27] A. Shimizu, Y. Tobe, *Angew. Chem. Int. Ed.* **2011**, *50*, 6906–6910; *Angew. Chem.* **2011**, *123*, 7038–7042.

[28] H. Miyoshi, S. Nobusue, A. Shimizu, I. Hisaki, M. Miyata, Y. Tobe, *Chem. Sci.* **2014**, *5*, 163–168.

[29] B. D. Rose, L. E. Shoer, M. R. Wasielewski, M. M. Haley, *Chem. Phys. Lett.* **2014**, *616-617*, 137–141.

[30] For comparison, the potential references were changed from Fc/Fc^+ to SCE, as described in: N. G. Connelly, W. Geiger, *Chem. Rev.* **1996**, *96*, 877–910.

[31] H. Reiss, A. Heller, *J. Phys. Chem.* **1985**, *89*, 4207–4213.

[32] a) Rahalkar, A.; Stanger, A. Aroma; http://chemistry.technion.ac.il/members/amnon-stanger/ (accessed 10/15/18); b) Stanger, A. *J. Org. Chem.* **2006**, *71*, 883–893; c) Stanger, A. *J. Org. Chem.* **2010**, *75*, 2281–2288; d) Gershoni-Poranne R; Stanger, A. *Chem. Eur. J.* **2014**, *20*, 5673–5688.

Entry for the Table of Contents

FULL PAPER

Containing an antiaromatic *as*-indacene as the core motif, a family of fully-conjugated indeno[2,1-*c*]fluorenes and related benzo-fused analogues has been prepared and fully characterized. The molecules possess high electron affinity and show a broad absorption that reaches into the near-IR region. The tropicity of the molecules has been probed by NICS-XY scan calculations.

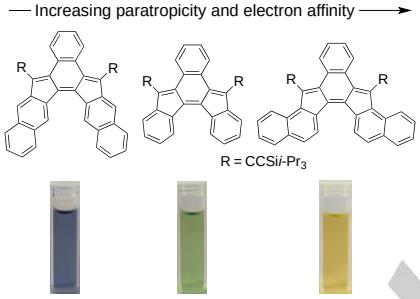

Tanguy Jousselin-Oba, Parker E. Deal, Aaron G. Fix, Conerd K. Frederickson, Chris L. Vonnegut, Abderrahim Yassar, Lev N. Zakharov, Michel Frigoli, and Michael M. Haley**

Page No. – Page No.

Synthesis and Properties of Indeno[2,1-*c*]fluorenes and Benzo-Fused Analogues

Supporting Information file

CIF file for cmpd 6a